Pulmonary Perfusion and Density Gradients in Healthy Volunteers

Helén M. Almquist, John Palmer, Björn Jonson and Per Wollmer
Departments of Clinical Physiology and Radiation Physics, University Hospital, Lund; and Department of Clinical Physiology, University Hospital MAS, Malmö, Sweden

The goal of this study was to measure regional pulmonary perfusion using SPECT and transmission tomography for attenuation correction and density measurements. **Methods:** Regional pulmonary perfusion was studied after intravenous injection of radiolabeled particles in 10 supine healthy volunteers using SPECT. Transmission tomography was used to correct for attenuation, measure lung density and delineate the lungs. The effects of attenuation correction on pulmonary perfusion gradients were investigated. **Results:** In perfusion measurements not corrected for attenuation, we found significant perfusion gradients in the direction of gravity but also significant gradients at isogravitational level. After correction for attenuation, the gravitational gradient was significantly greater than before correction, and gradients at isogravitational level were no longer observed. Perfusion in the ventral lung zone was half of that in the dorsal lung zone. Mean lung density was 0.28 ± 0.03 g/ml, and density showed a significant increase in the direction of gravity and at isogravitational level. **Conclusion:** We found that SPECT perfusion studies of the lung not corrected for attenuation gave a false impression of nongravitational gradients and underestimate the gradient that is gravity-dependent. Transmission tomography, used for attenuation correction, also quantifies lung density and shows gravity dependent and nondependent density gradients.

Key Words: pulmonary circulation, attenuation correction, transmission tomography, SPECT

J Nucl Med 1997; 38:962–966

Regional blood flow in the normal human lung has a nonuniform distribution. West et al. (*1*) demonstrated a large increase in regional blood flow in the direction of gravity and subsequently presented a model for gravitational effects on intravascular blood pressure and flow. Early studies of the distribution of pulmonary blood flow in man relied on the use of radioactive gases and scintillation probes placed over the chest. Perfusion gradients in the human lung have, in recent years, been the subject of two studies using SPECT technique (*2,3*), which makes it possible to study the distribution of radioactivity in three directions with much improved resolution. These studies showed the gravity dependent perfusion gradient to be less pronounced than would be expected from previous studies and also indicated the presence of nongravity dependent perfusion. Technical factors may affect the result of measurements of the distribution of radioactivity in the lungs. The finite resolution of tomographic detector systems makes delineation of the lung difficult. In a reconstructed plane, there will be a gradual reduction in count density at the edge of the lung, which may simulate a perfusion gradient. Photons emitted from the lungs are subject to variable attenuation, resulting in loss of photons and misplacement of detected scattered photons (build-up). The effect of attenuation was not considered in previous SPECT studies of regional pulmonary perfusion in man (*2,3*). The primary goal of this study was, therefore, to measure the distribution of pulmonary blood flow in normal man with SPECT, using appropriate correction for attenuation and build-up of scattered photons, in accordance with our previous report (*4*). The transmission measurement, used to correct for attenuation and to delineate the lungs, also provides information about the regional density of the lung. Another aim was to study the regional distribution of lung density. We studied differences between analysis based on manually selected two-dimensional data and operator independent three-dimensional analysis.

Received Apr. 8, 1996; revision accepted Oct. 8, 1996.
For correspondence or reprints contact: Helén M. Almquist, MD, Department of Clinical Physiology, University Hospital, S-221 85 Lund, Sweden.

MATERIALS AND METHODS

Ten healthy nonsmoking volunteers (9 men, 1 woman; age range 41–55 yr; mean age 46.5 yr) were studied. The subjects had no history of lung disease. They had values of slow vital capacity (VC) and forced expiratory volume in one second (FEV_{1s}) within normal limits (*5*). The study was approved by the Research Ethics Committee of the Medical Faculty, Lund University, and informed consent was obtained from each subject.

The subject was in the supine position, arms above the head, breathing quietly during the scintigraphic studies. A 35 × 50 cm field of view gamma camera was used, equipped with a low-energy, general purpose collimator, modified to support a transmission flood source with approximately 500 MBq of ^{99m}Tc-pertechnetate at a distance of 40 cm from the camera head. Acquisition parameters were 64 × 64 matrix, 72 frames over 360°, pixel size of 5.33 mm and acquisition time 24 min.

Transmission tomography was performed with and without the subject and examination couch positioned in the field of view. These data were used to generate a density projection set from which density maps were reconstructed. After the flood source had been removed, 75 MBq ^{99m}Tc-labeled macroaggregated albumin (^{99m}Tc-MAA) was injected intravenously without repositioning the subject, and the perfusion (emission) study was performed according to the same protocol. The emission projection data were then corrected by multiplicative factors before final reconstruction. These factors were obtained from a preliminary reconstruction, from which projections were simulated with the assumption of no attenuation, as well as with the attenuation implied by the previously obtained attenuation maps. The pixel-wise quotient of these two simulated projections yielded the required correction factors. The method has been previously described (*4*).

For perfusion and density data both two- and three-dimensional analysis was performed, with focus on the right lung because of its larger size and accordingly lower degree of edge effects. Two-dimensional analysis of gravity dependent, ventrodorsal gradients was performed in a transverse plane 8 cm above the top of the diaphragmatic dome. Analysis of nongravity dependent, apicobasal gradients was performed in a coronal plane through the central part of the lung. The slice thickness was 2.1 cm. Perfusion and density profiles were obtained from regions of interest (ROI), 2.1 × 2.1

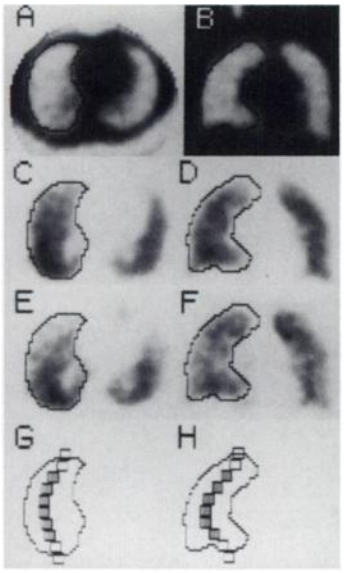

FIGURE 1. Transversal (A,C,E) and coronal (B,D,F) slices showing lung density (A and B), uncorrected perfusion (C and D) and corrected perfusion (E and F). The contour represents the density limit, 0.58 g ml^{-1}, of the right lung and its relation to the ROIs forming the profiles, is shown in G and H. The contour also illustrates the border of the total volume representing lung tissue, i.e., the PXtot, as represented in this slice. The ROIs included in the two-dimensional analysis, the ROIres, are shaded.

cm, manually placed across the lung field (Fig. 1 panel G and H). Hilar structures were avoided. ROIs with a density value of 0.58 g/ml or less were considered to represent lung tissue, as indicated by a separate phantom study with known densities. These ROIs were subsequently transferred to the emission study for analysis of perfusion gradients. The outermost ROI in each direction was excluded to avoid edge effects. The remaining ROIs, forming a restricted profile, were denoted ROIres. Linear regression was applied to the ROIres of each individual profile. Density gradients were expressed as gram/milliliter per centimeter. As perfusion was only measured in relative terms, perfusion gradients were expressed in percent of the value at the midpoint of each profile obtained from the ROIres (%/cm). Individual mean density values were calculated using the same ROIres and expressed as g/ml.

The three-dimensional analysis was automatic. A total volume of pixels with a density value of 0.58 g/ml or less denoted PXtot (Fig. 1) and was considered to represent lung tissue. To avoid edge effects a zone of two pixels along the lung border was excluded, leaving a restricted volume of pixels called PXres. A separate analysis preceded the choice of the two pixels wide zone: the consequence of masking off an up to five pixels wide peripheral zone was studied using first and second degree multiple regression equations to fit the perfusion data in three dimensions. An indicator of the nonlinearity of the data, the Laplacian ($\Sigma d^2/dx_i^2$), was minimized in magnitude at a mask of approximately two pixels. Differences between the linear terms of the first and second degree equations were small in all three directions. Multiple linear regression was therefore applied to the PXres to calculate density and perfusion gradients avoiding edge effects. A first degree regression equation was used:

$$p = c_0 + c_{ml}X + c_{vd}Y + c_{ab}Z,$$

where p is density or relative perfusion, X, Y and Z are the spatial coordinates; c_{ml}, c_{vd} and c_{ab} are gradients in the mediolateral, the ventrodorsal and apicobasal directions. The calculated value at the origin of the coordinate system, c_0, located in the midpoint of the PXtot, was referred to as the central value. Perfusion gradients, calculated using multiple linear regression, were expressed as percent of central value per cm (%/cm). Individual mean density, expressed as g/ml thorax, was calculated for the total and the restricted lung volume, i.e., the PXtot and the PXres.

Results are given as overall group mean with one s.d. Individual gradients, i.e., regression coefficients of perfusion or density were used as summary measures according to Matthews et al. (*6*) implying that group mean values were analyzed with Student's t-test and differences between means with paired Student's t-test (two-tailed in both cases). Significance of individual gradients were tested using the F-test. The degrees of freedom in the three-dimensional analysis were reduced by applying the F-test to several observations representing a volume element of size (2.1 $cm)^3$. This corresponds approximately to the image resolution. $p < 0.05$ was regarded as significant.

RESULTS

Pulmonary Perfusion

Perfusion tomograms not corrected for attenuation showed higher counts in the dorsal than in the ventral part (Fig. 1, panel C) and relatively low counts in the apical part (Fig. 1, panel D), suggesting a ventrodorsal and an apicobasal perfusion gradient. After correction, the difference between counts in the ventral and dorsal part increased (Fig. 1, compare panel C and E), while the difference has decreased between the apical and basal parts (Fig. 1, compare panel D and F). These observations are reflected in the two-dimensional profiles (Fig. 2). Before attenuation correction two-dimensional analysis showed significant gradients in both the ventrodorsal and apicobasal direction (Table 1). After correction, this was only found in the ventrodorsal direction, where the mean gradient was significantly higher, 5.2%/cm. Three-dimensional analysis, before correction, showed significant gradients in all three directions but after correction only in the ventrodorsal direction. The mean ventrodorsal gradient thus shown was 5.0%/cm, i.e., very similar as in the two-dimensional analysis. It was also significant in each individual in the three-dimensional analysis but not in two-dimensional analysis where the individual with the smallest lung in this direction did not have a significant gradient.

Lung Density

In density tomograms a gradient in the ventrodorsal (gravitational) direction but not in the apicobasal direction was clearly seen (Fig. 1, panel A and B). The statistical two-dimensional analysis of regional density distribution showed a highly significant increase in lung density towards dependent lung regions (Table 2), also illustrated in Figure 3. In addition, a smaller increase in density from base to apex was found (Table 2). Three-dimensional analysis showed significant gradients in all three directions but in the apicobasal direction with an opposite direction compared to the two-dimensional analysis. The ventrodorsal gradient shown with three-dimensional analysis was 0.007 g/ml per cm and it did not differ significantly between three- and two-dimensional analysis.

Mean lung density was presented in relation to the individual lung size within the PXtot. The group mean density of the ROIres of the 10 subjects were equal in the ventrodorsal and apicobasal directions (Fig. 4A) and on average 0.28 ± 0.03 g/ml. The smallest lung deviated most from this value. In three-dimensional analysis density calculated for the PXres increased with decreasing lung size (Fig. 4B). The relationship is described by: density = $-0.06 \times$ lung size + 0.41 ($r = 0.84$, $p < 0.01$). Lung density calculated for the PXtot was for each lung higher than that for the PXres. The difference was 0.07 ± 0.005 g/ml ($p < 0.01$).

DISCUSSION

This study demonstrates that SPECT studies of the distribution of pulmonary perfusion in normal man yield significant perfusion gradients in the direction of gravity as well as in isogravitational directions if correction for attenuation and

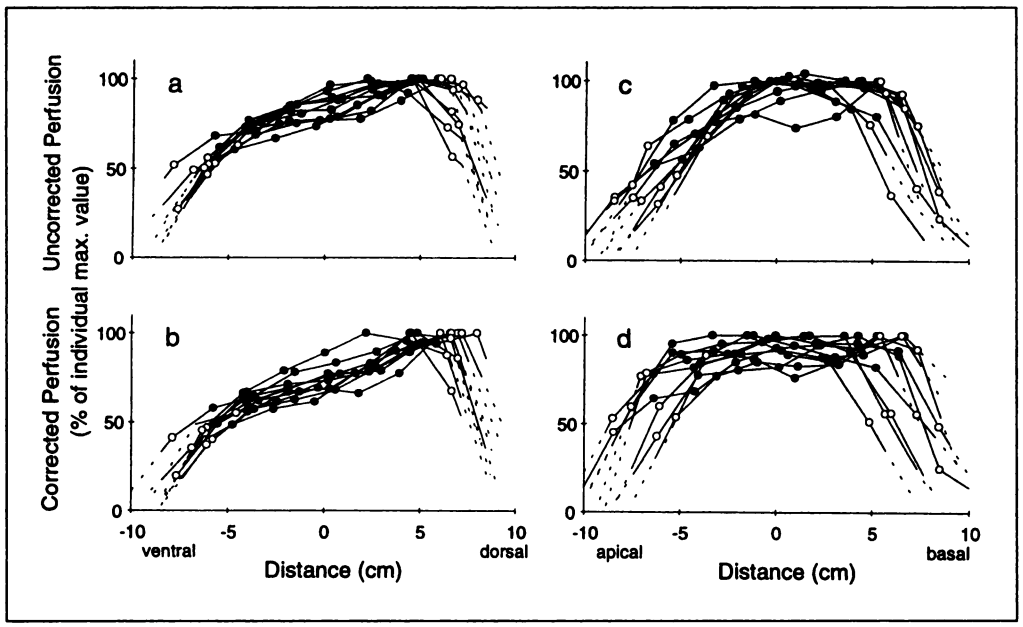

FIGURE 2. Ventrodorsal distribution of lung perfusion, uncorrected (a) and corrected data (b). Apicobasal distribution of lung perfusion, uncorrected (c) and corrected data (d). Dotted lines represent data exterior to the 0.58 g/ml border. Circles (● and ○) represent mean ROI values. The ROIs included in the two-dimensional analysis, the ROIres, are indicated by closed circles (●).

buildup is not used. After such corrections, a significant gradient remains in the direction of gravity only. The differences between our results and previous reports are likely to be explained by effects of attenuation and scatter and by the use of different methods for delineating the lungs. From emission measurements alone, it is extremely difficult, if at all possible, to differentiate between edge effects and a physiological gradient of reduced blood flow towards the lung periphery.

Nongravity dependent perfusion gradients have been reported in the normal human lung in SPECT studies by Hakim et al. (*2*) and Orphanidou et al. (*3*) as well as gravity dependent gradients. The values of the gradients found by Orphanidou et al. (*3*) were of the same magnitude as our values but with a negative apicobasal gradient. A concentric perfusion pattern with higher perfusion in the center than in the periphery of the lung, reported by Hakim et al. (*2*), is expected from their method of delineation, only excluded counts below 10% of the maximal value. Gravity dependent perfusion gradients of the same order as our results were also reported by Maeda et al. (*7*) in a SPECT study wihtout attenuation correction. The authors indicate that these gradients are calculated excluding the periphery of the lungs. They also reported uniform distribution of perfusion in the nongravity direction, though numerical data was not given.

Brudin et al. (*8*) using PET, including attenuation correction, found a significant perfusion gradient only in the ventrodorsal, gravity dependent direction and no gravity independent perfusion gradients. As in our study, the lung was delineated by a thresholding procedure using a density study. In the most dorsal part of the lung the value of the perfusion gradient was higher than our results, possibly because perfusion was calculated from measured ventilation and ventilation/perfusion-ratios. Attenuation corrected SPECT images of human pulmonary perfusion have been presented (*9,10*) but without analysis of perfusion gradients. Recently, Damen et al. (*11*) reported low relative perfusion near the apex of the lung in supine subjects in a SPECT study. They used radiograph CT for lung delineation and attenuation correction. Edge effects were not discussed.

To obtain a correct density value from SPECT, only the central part of the lung can be considered. Thus, the value calculated is in accordance with density values obtained using PET (*12–14*). In studies of lung pathology, it may be desirable to measure lung density in a larger portion of the lung. The mean values should then be interpreted in relation to the size of the lung studied. The reason for the higher values obtained for the smaller lungs may be biological or technical. A larger lung is characterized by larger alveoli and hence per volume less alveolar and interstitial structures (*15*). Residual edge effects can also have contributed to our values.

The value of the density gradient obtained in the gravity-dependent ventrodorsal direction is of the same magnitude as the gravity dependent gradients obtained by PET, explained by both increased blood volume and lung tissue volume per cm^3 of thoracic volume (*12*).

TABLE 1
Perfusion Gradients

	Ventrodorsal (%/cm)	Apicobasal (%/cm)	Mediolateral (%/cm)
	Two-dimensional analysis		
Uncorrected	3.6 ± 0.9*‡	2.6 ± 1.7*§	
Corrected	5.2 ± 1.2*	0.5 ± 1.9	
	Three-dimensional analysis		
Uncorrected	2.8 ± 1.2*‡	1.4 ± 1.6†§	2.4 ± 2.4†‡
Corrected	5.0 ± 1.2*	1.0 ± 1.7	−1.1 ± 2.3

*Significant perfusion gradient, $p < 0.001$.
†Significant perfusion gradient, $p < 0.05$.
‡Significantly different from corrected value, $p < 0.001$.
§Significantly different from corrected value, $p < 0.01$.
Values are mean ± s.d.

TABLE 2
Density Gradients

Ventrodorsal (g/ml per cm)	Apicobasal (g/ml per cm)	Mediolateral (g/ml per cm)
	Two-dimensional analysis	
0.008 ± 0.004*	−0.005 ± 0.005*†	
	Three-dimensional analysis	
0.007 ± 0.002*	0.005 ± 0.002*‡	−0.011 ± 0.003*

*Significant density gradient, $p < 0.001$.
†Significant density gradient, $p < 0.01$.
‡Significantly different from corrected value, $p < 0.001$.
Values are mean ± s.d.

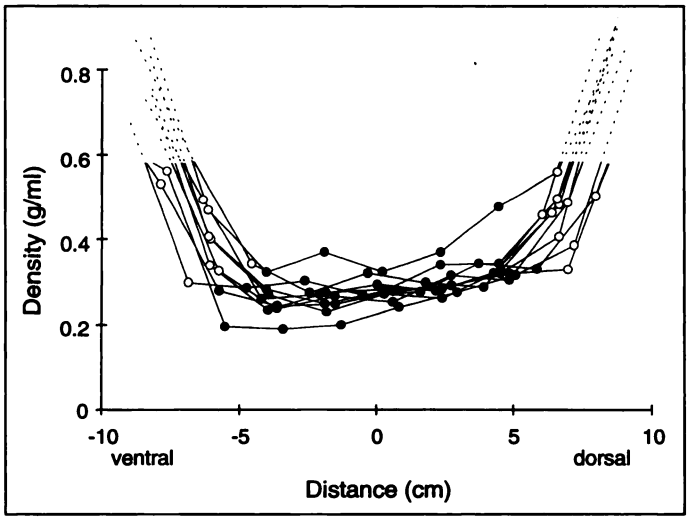

FIGURE 3. Ventrodorsal distribution of density of the right lung. Dotted lines represent data exterior to the 0.58 g/ml border. Circles (● and ○) represent mean ROI values. The ROIs included in the two-dimensional analysis, the ROIres, are indicated by closed circles (●).

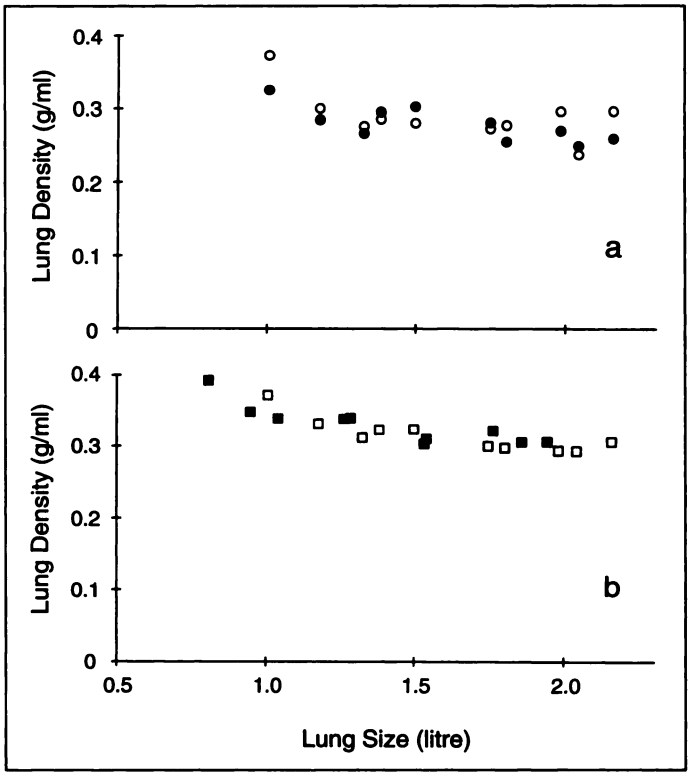

FIGURE 4. (a) Mean lung density of the right lung, calculated from ROI profiles in the ventrodorsal (●) and apicobasal (○) direction, as a function of lung size. (b) Mean lung density for the left (■) and right (□) lung, calculated for the restricted lung volume, i.e., the PXres, as a function of lung size.

In general, the group mean gradients we obtained by two-dimensional analysis were consistent with those obtained by three-dimensional analysis. The only exception found was the density variation from apex to base, where the two-dimensional and three-dimensional analysis gave gradients of opposite directions. The two-dimensional analysis includes a subjective selection of ROI, where apical ROI often are more medial, and thus denser, than basal ROI giving a decrease in density from apex to base. With three-dimensional analysis, where the whole body of information is used, density instead increases towards the base. An explanation for the higher density at the lung base is the cranial displacement of the diaphragm in the supine position, causing lung deformation. The higher density in the medial than in the lateral regions of the lung, could be due to interstitial structures, vessels and bronchi radiating from the center to the periphery.

That SPECT is superior to planar imaging in studies of regional pulmonary perfusion was first demonstrated by Osborne et al. (*16*). The impact of attenuation on pulmonary perfusion studied using SPECT is considerable, as this study demonstrates for perfusion gradients. None the less, compensation for attenuation has not been commonly used.

CONCLUSION

With the introduction of multihead gamma cameras, SPECT studies are becoming clinically more feasible, as is attenuation correction by means of transmission measurements, using equipment for simultaneous emission and transmission. This also offers the possibility to obtain an exact anatomical correlation between perfusion and density, which is of potential clinical value. We have found that uncorrected perfusion SPECT studies give a false impression of nongravitational gradients and underestimate the gradient that is gravity-dependent. Due to the limited resolution of the scintillation cameras, a perfusion gradient existing only in the periphery of the lung may not have been detected. Both perfusion and density gradients are best studied using three-dimensional analysis, as two-dimensional analysis is subject to variation due to the investigators choice of regions to include in the analysis. Three-dimensional analysis is operator-independent, estimates overall gradients and is possible to perform automatically. In practice, SPECT is the only method that allows such three-dimensional analysis.

ACKNOWLEDGMENTS

This study was supported by the National Association Against Chest and Heart Diseases, by the Swedish Medical Research Council grant 02872, by the Gorton Foundation in Helsingborg and by the Medical Faculty of Lund University.

REFERENCES

1. West JB, Dollery CT, Naimark A. Distribution of blood flow in isolated lung: relation to vascular and alveolar pressures. *J Appl Physiol* 1964;19:713–724.
2. Hakim TS, Lisbona R, Dean GW. Gravity independent inequality in pulmonary blood flow in humans. *J Appl Physiol* 1987;63:1114–1121.
3. Orphanidou D, Hughes JMB, Myers MJ, Al-Suhali AR, Henderson B. Tomography of regional ventilation and perfusion using krypton 81m in normal subjects and asthmatic patients. *Thorax* 1986;41:542–551.
4. Almquist, H, Palmer J, Ljungberg M, Wollmer P, Strand SE, Jonson B. Quantitative SPECT by attenuation correction of the projection set using transmission data: evaluation of a method. *Eur J Nucl Med* 1990;16:587–594.
5. Berglund E, Birath G, Bjure J, et al. Spirometric studies in normal subjects. Forced expirograms in subjects between 7 and 70 yr of age. *Acta Med Scand* 1963;173:185–192.
6. Matthews JNS, Altman DG, Campbell MJ, Royston P. Analysis of serial measurements in medical research. *Br Med J* 1990;300:230–235.
7. Maeda H, Itoh H, Ishii Y, et al. Pulmonary blood flow distribution measured by radionuclide computed tomography. *J Appl Physiol* 1983;54:225–233.
8. Brudin LH, Rhodes CG, Valind SO, Jones T, Hughes JMB. Interrelationship between blood flow, blood volume and ventilation in supine man. *J Appl Physiol* 1994;76:1205–1241.
9. Bailey DL, Hutton BF, Walker PJ. Improved SPECT using simultaneous emission and transmission tomography. *J Nucl Med* 1987;28:844–851.
10. Tan P, Bailey DL, Meikle SR, Eberl S, Fulton RR, Hutton BF. A scanning line source for simultaneous emission and transmission measurements in SPECT. *J Nucl Med* 1993;34:1752–1760.
11. Damen EMF, Muller SH, Boersma LJ, de Boer RW, Lepesque JV. Quantifying local lung perfusion and ventilation using correlated SPECT and CT data. *J Nucl Med* 1994;35:784–792.

12. Brudin LH, Rhodes CG, Valind SO, Wollmer P, Hughes JMB. Regional lung density and blood volume in nonsmoking and smoking subjects measured by PET. *J Appl Physiol* 1987;64:1324–1334.
13. Rhodes CG, Wollmer P, Fazio F, Jones T. Quantitative measurement of regional extravascular lung density using positron emission and transmission tomography. *J Comput Assist Tomogr* 1981;5:783–791.
14. Wollmer P, Rhodes CG, Allan RM, Maseri A, Fazio F. Regional extravascular lung density and fractional pulmonary blood volume in patients with chronic pulmonary venous hypertension. *Clin Physiol* 1983;3:241–256.
15. Weibel ER, Gomez DM. Architecture of the human lung. *Science* 1962;137:577–585.
16. Osborne D, Jaszczak R, Coleman RE, Drayer B. Single-photon emission computed tomography in canine lung. *J Comput Assist Tomogr* 1981;5:684–689.

Impaired Permeability in Radiation-Induced Lung Injury Detected by Technetium-99m-DTPA Lung Clearance

Herbert Susskind, David A. Weber, Yat Hong Lau, Tae L. Park, Harold L. Atkins, Dinko Franceschi, Allen G. Meek, Marija Ivanovic and Lucian Wielopolski

Clinical Research Center, Brookhaven National Laboratory, Upton, New York; Department of Radiation Oncology, University Hospital, SUNY-Stony Brook, Stony Brook, New York

This study evaluates the use of the ^{99m}Tc-DTPA aerosol lung clearance method to investigate radiation-induced lung changes in eight patients undergoing radiotherapy for lung or breast carcinoma. The sensitivity of the method was compared with chest radiography for detecting radiation-induced changes in the lung, regional alterations within (irradiated region) and outside (shielded region) the treatment ports, effect of irradiated lung volume, and dependence on time after radiotherapy. **Methods:** Serial DTPA lung clearance studies were performed before the first radiation treatment (baseline), then weekly during a 5- to 7-wk course, and up to 12 times post-therapy over periods of 56–574 days. The total activity deposited in the lungs for each study was ~150 μCi (~5.6 MBq). DTPA clearance, expressed in terms of the biological half-time, $t_{1/2}$, was computed from the slopes of the least-squares fit regression lines of the time-activity curves for the first 10 min for irradiated and shielded lung regions. **Results:** Major findings include: (a) significant and early DTPA $t_{1/2}$ changes were observed in all patients during and after radiotherapy; (b) changes in DTPA $t_{1/2}$ values were observed in both irradiated and shielded lung regions in all patients suggesting a radiation-induced systemic reaction; (c) changes in DTPA $t_{1/2}$ values were correlated ($p < 0.05$) with the irradiated lung volumes; (d) significantly reduced DTPA $t_{1/2}$ values were observed in three patients who subsequently presented with clinical symptoms and/or radiographic changes consistent with radiation pneumonitis ($t_{1/2}$ fell to 19% ± 6% of baseline values, compared with 64% ± 17% in the remaining patients [$p < 0.01$]); (e) the onset of decreased DTPA $t_{1/2}$ values in these three patients occurred 35–84 days before clinical symptoms and/or radiographic changes; and (f) DTPA $t_{1/2}$ tended to approach baseline values with time after radiotherapy, suggesting a long-term recovery in lung injury. **Conclusion:** These observations show significant and early alterations in DTPA lung clearance during and after radiotherapy that may provide a sensitive assay to monitor changes in radiation-induced lung injury and may facilitate early therapeutic intervention.

Key Words: radiation-induced lung injury; radiation pneumonitis; radiotherapy; technetium-99m-DTPA; lung clearance

J Nucl Med 1997; 38:966–971

Radiation-induced injury to the lungs is a potential side effect in the radiation treatment of tumors in the chest. Radiation pneumonitis presents clinically with dry cough, dyspnea and fever. Chest radiographs often reveal an infiltrate, characteristically within the radiation port. Radiation pneumonitis may subside, leaving no clinical or radiological traces, or progress slowly to irreversible chronic pulmonary fibrosis (*1,2*). Symptomatic pneumonitis and/or fibrosis occur in 5%–20% of patients irradiated for carcinoma of the lung or breast (*3,4*). Chest radiographs show that an even larger percentage of patients develop subclinical pulmonary injury (*3*).

Diagnostic procedures used previously for the detection of radiation-induced lung injury include the measurement of ^{67}Ga citrate uptake in inflammatory lung tissue (*5,6*), analysis of bronchoalveolar lavage (BAL) fluid for inflammatory cells in the lung air spaces (*7–11*), measurement of regional lung ventilation and perfusion (*12*), MR imaging (*13*), and chest radiographs (*14*) and CT scans (*15*). The usefulness and number of serial studies that can be performed are limited for each of these procedures. Gallium is limited by the high total-body radiation dose of 780 mrad (7.8 mGy) for a 3 mCi (111 MBq) dose and a 72-hr waiting time between administration to the patient and imaging. BAL is limited by trauma and discomfort to the patient; lung ventilation and perfusion measurement by the relatively high lung radiation dose of 920 mrad (9.2 mGy) for a 4 mCi (148 MBq) dose. MR imaging is limited by study cost and chest radiographs and CT scans are limited by their marginal sensitivity.

In this study, the rate of lung clearance of inhaled ^{99m}Tc-labeled diethylenetriamine pentaacetate aerosol (DTPA), a sensitive index of lung epithelial permeability (*16*), was used to measure changes in the permeability of the alveolar-capillary membrane of patients receiving radiation to the lung for treatment of lung or breast carcinomas. The method is based on the deposition of inhaled DTPA particles on the alveolar epithelial surface, followed by their diffusion through the alveolar-capillary membrane, solution in capillary blood and excretion through the kidneys. The radiation beam may cause an inflammation, thereby increasing epithelial permeability and resulting in faster DTPA clearance, expressed as a reduced biological clearance half-time, $t_{1/2}$. Conversely, the radiation beam may cause the formation of hyaline membranes and the deposition of macrophages and other cells and exudates on the epithelium, thereby lengthening the DTPA diffusion path and decreasing DTPA clearance, expressed as an increased $t_{1/2}$. The procedure is very attractive because it is noninvasive, very

Received May 24, 1996; revision accepted Oct. 30, 1996.
For correspondence or reprints contact: Herbert Susskind, PE, Clinical Research Center, Brookhaven National Laboratory, Box 5000, Upton, NY 11973-5000.